Posted on Authorea 21 Jul 2020 — The copyright holder is the author/funder. All rights reserved. No reuse without permission. — https://doi.org/10.22541/au.159534893.31472268 — This a preprint and has not been peer reviewed. Data may be preliminary.

Metabolic flux from the chloroplast provides signals controlling photosynthetic acclimation to cold in Arabidopsis thaliana.

Helena Herrmann[1], Beth Dyson[2], Matthew Miller[1], Jean Marc Schwartz[1], and Giles Johnson[1]

[1]University of Manchester
[2]University of Sheffield

July 21, 2020

Abstract

Photosynthesis is especially sensitive to environmental conditions and the composition of the photosynthetic apparatus can be modulated in response to environmental change, a process termed photosynthetic acclimation. Previously, we identified a role for a cytosolic fumarase, FUM2 in acclimation to low temperature in Arabidopsis thaliana. Mutant lines lacking FUM2 were unable to acclimate their photosynthetic apparatus to cold. Here, using gas exchange measurements and metabolite assays of acclimating and non-acclimating plants, we show that acclimation to low temperature results in a change in the distribution of photosynthetically fixed carbon to different storage pools during the day. Proteomic analysis of wild-type Col-0 Arabidopsis and of a fum2 mutant which was unable to acclimate to cold indicates that extensive changes occurring in response to cold are affected in the mutant. Metabolic and proteomic data were used to parameterise metabolic models. Using an approach called flux sampling, we show how the relative export of triose phosphate and 3-phsphoglycerate provides a signal of the chloroplast redox state that could underly photosynthetic acclimation to cold.

Introduction

Through their lifecycle, plants experience environmental conditions that vary on timescales from seconds to seasons. *Arabidopsis thaliana*is typically a winter annual, germinating in the autumn and persisting through the winter, prior to flowering in spring (Grime*et al.* , 1988). Across this time-period, mean daily temperatures may vary by 20°C or more. To optimise survival and growth, plants acclimate to changes in temperature, altering their investment in different processes to suit the conditions experienced (Ruelland, Vaultier, Zachowski, & Hurry, 2009; Walters, 2005). The process of acclimation can involve both structural changes, with tissues differing when developed in different conditions, and relatively rapid (days-weeks) dynamic responses, which track changes in the environment (Athanasiou, Dyson, Webster, & Johnson, 2010; Walters, 2005). Changes in light intensity and temperature are both known to trigger acclimation (Athanasiou *et al.* , 2010; Dyson *et al.* , 2015; Dyson*et al.* , 2016; Huner *et al.* , 1993; Savitch *et al.* , 2001; Stitt & Hurry, 2002; Strand, Hurry, Gustafsson, & Gardestrom, 1997; Walters & Horton, 1994).

Exposure to low temperature triggers a complex array of acclimation responses. A significant amount of work in plant cold responses has focused on the acquisition of freezing tolerance (see Knight & Knight, 2012 for a review). In addition, it is recognised that plants can optimise their metabolism to suit changing conditions. For example, both photosynthesis (Huner *et al.* , 1993; Strand *et al.* , 1997; Strand *et al.* , 1999) and respiration (Armstrong, Logan, Tobin, O'Toole, & Atkin, 2006; Talts, Pärnik, Gardeström, & Keerberg, 2004) can readily be measured in intact leaves so it is easy to follow acclimation of these processes *in vivo* . A prominent feature of metabolic acclimation is an increase in the capacity of metabolism, with enzyme and metabolite concentrations increasing to compensate for the loss of activity at low temperature (Savitch

Posted on Authorea 21 Jul 2020 — The copyright holder is the author/funder. All rights reserved. No reuse without permission. — https://doi.org/10.22541/au.159534893.31472268 — This a preprint and has not been peer reviewed. Data may be preliminary.

et al. , 2001; Savitch *et al.* , 2002; Stitt & Hurry, 2002). This requires the coordination of gene expression across multiple cellular compartments, including retrograde and/or anterograde signals between the nucleus, chloroplast and mitochondrion (Fey, Wagner, Brautigam, & Pfannschmidt, 2005). To date, little is known about either the sensing or the signalling pathways involved in metabolic acclimation.

Acclimation of photosynthesis to low temperature has previously been studied in a range of species, including Arabidopsis. In the short term, low temperature decreases the rate at which sucrose is synthesised and exported from the leaf. Limitations in flux through sucrose phosphate synthase (SPS) result in the accumulation of phosphorylated metabolites (Hurry, Strand, Furbank, & Stitt, 2000). This is thought to lead to depletion of the cellular concentration of inorganic phosphate (Pi) which in turn limits the export of triose phosphate (TP) from the chloroplast. This inhibits photosynthesis, as the regeneration of Pi in the chloroplast is necessary for ATP synthesis. Over relatively short periods (days) increased expression of SPS removes the limitation in sucrose synthesis. Hurry et al. (2000) proposed, based on the responses of different mutants with altered phosphate content, that Pi depletion provides a signal for cold acclimation of SPS content.

Recently, we re-examined the responses of Arabidopsis to low temperature (Dyson*et al.* , 2016). Using non-targeted metabolomics, we identified the diel accumulation of the organic acid fumaric acid (predominantly present in the anionic form, fumarate) as important in the response to cold. We showed that the accumulation of fumarate, which requires the presence of a cytosolic isoform of the enzyme fumarase, FUM2 (Pracharoenwattana*et al.* , 2010), is a specific response to temperature. Plants of two independent mutant lines lacking this enzyme not only failed to accumulate fumarate over the photoperiod, they also accumulated*higher* concentrations of phosphorylated intermediates. Crucially, whilst wild-type Col-0 Arabidopsis plants increase photosynthetic capacity in response to low temperature, *fum2* mutant plants do not. This suggests that Pi deficiency alone is not sufficient to trigger photosynthetic acclimation.

Here, we have used a combined metabolic and proteomic approach, together with physiological analyses to dissect the acclimation processes occurring in Arabidopsis in response to low temperature. We focus on dynamic acclimation responses to cold in leaves developed at higher temperature. Our results show that fumarate accumulation is important for a wide range of metabolic acclimation responses to cold. Our beginning- and end-of-day measurements of carbon pools indicate that there is a shift from day- to night-time carbon consumption upon cold acclimation. Furthermore, based on results from metabolic modelling constrained using experimental data, we propose that changes in the pathway of carbohydrate export from the chloroplast link to fumarate accumulation at low temperature and provide a mechanism controlling photosynthetic acclimation to cold.

Materials and Methods

Plant material and growth

Wild-type Col-0 seeds were obtained from the Nottingham Arabidopsis Stock Centre. Seeds possessing insertions in the gene At5g50950 (*fum2.1* and *fum2.2*) encoding cytosolic FUM2 protein (Pracharoenwattana *et al.* , 2010) were kindly provided by Professor Steven Smith (University of Tasmania, Australia). Plants were grown in 3" pots containing peat-based multipurpose compost, in an SGC120 growth cabinet (Weiss Technik) with an 8-h photoperiod, to supress flowering, at a temperature of 20°C day/16°C night, and irradiance of 100 μmol m^{-2} s^{-1}provided by warm white fluorescent tubes for 8 weeks in 3-inch pots containing peat-based compost. After 8 weeks, plants had reached growth stage 1.10 (Boyes *et al.* , 2001), with more than 10 leaves > 1 mm and persisted without development of flowers until 10 to 12 weeks. Plants for cold treatment were transferred to a similar cabinet at 4°C day/night 1 h prior to the start of the photoperiod. Leaves for metabolite measurements were harvested by flash freezing in liquid nitrogen under growth conditions.

Estimation of seed yield

8-week-old wild-type Col-0 and *fum2.2* plants were kept in control conditions or were cold treated for 1 week as described above. Plants were then moved to a growth chamber with a 16-hour daylength, 20°C, to trigger flowering. After a further 8 weeks, the number of siliques per plant was counted on 6 plants for

Posted on Authorea 21 Jul 2020 — The copyright holder is the author/funder. All rights reserved. No reuse without permission. — https://doi.org/10.22541/au.159534893.31472268 — This a preprint and has not been peer reviewed. Data may be preliminary.

each treatment group and the number of seeds silique pod was estimated for 10 individual siliques per plant. Total seed yield was estimated as the product of silique number and mean seeds per silique.

Measurements of photosynthesis and respiration

Measurements of photosynthetic capacity were made using a LiCor LI-6400 infra-red gas analyser, at a temperature of 20°C in an atmosphere of 2000 µl l^{-1} CO_2 flow rate 200 $cm^{-3}.min^{-1}$, and an irradiance of 2000 µmol m^{-2} s^{-1} provided by a warm white LED (colour temperature 2800–3200 K). Leaves were illuminated for 30 mins to fully induce photosynthesis before a measurement was recorded. The light was then switched off to allow an estimate of the dark rate of gas exchange. Measurements of photosynthesis and respiration under growth conditions were carried out using the same gas analyser, in the growth cabinet where plants were grown, using ambient air conditions. The gas analyser was placed in the cabinet and allowed to equilibrate for at least 1 hour prior to any measurements. The analyser chamber was placed to give a light intensity in the chamber equivalent to that of plants during growth. Respiration was measured by interrupting illumination, covering the plant and analyser chamber with aluminium foil. All measurements were performed between the 5^{th} and 6^{th} hour of the photoperiod. Data were analysed using an analysis of variance, followed by a Tukey post-hoc tests in SPSS (IBM).

Enzyme-Linked Assays of Metabolites

Enzymatic assays were carried out on extracts from fully expanded leaves as described previously (Dyson *et al.* , 2016). Starch, sucrose and glucose, and malate were measured using total starch (Method E), sucrose D-glucose, and l-malic acid assay kits (Megazyme), respectively. To measure fumarate, the malate kit was modified to include an extra independent reaction step, using 2 units of fumarate hydratase enzyme (Sigma). Data were analysed using an analysis of variance, followed by a Tukey post-hoc test, in SPSS (IBM).

Proteomic analysis of plant material

Extraction of leaf proteins and analysis of protein content using gel-free LC-MS/MS was carried out as described by Miller *et al.*(2017). Briefly, frozen ground leaf samples (4 replicates per treatment) were extracted in a buffer containing Rapigest. After reduction, alkylation and trypsin digestion, samples were analysed by LC-MS/MS using an UltiMate® 3000 Rapid Separation LC (RSLC, Dionex Corporation, Sunnyvale, CA) coupled to an Orbitrap Elite mass spectrometer (Thermo Fisher Scientific, MA, USA). Raw data were imported into Progenesis QI (build 2.0.5556.29015; Nonlinear Dynamics, Newcastle, United Kingdom) and runs were aligned according to the default settings. Only ions with a charge state of up to +4 were considered. MS/MS data were searched against the *A. thaliana* TAIR 10 database and assigned to peptides using Mascot version 2.4.0 (Matrix Science, London, United Kingdom). A maximum of one missed cleavage (Trypsin) was permitted, with a peptide mass tolerance of 10 ppm and an MS/MS tolerance of 0.5 Da. Data were then re-imported into Progenesis to allow for assignment of proteins from peptide data. Raw protein intensities were then exported from Progenesis and normalised to the sample with the median total protein content for that treatment, as described previously (Miller *et al.* , 2017). Total protein for each sample was calculated by summing the intensities of all the quantified proteins.

A principal component analysis (PCA) was performed in the R software package using log2 scaled protein intensities using the pcaMethods R package. The "svd" function was used, and 10 principal components were included in the calculation. Proteins were considered to have significantly changed in abundance when a p value of <0.05 was reached, with a fold change of 1.2 or greater. For hierarchical clustering analysis, $\log_2$ scaled protein values were used. Hierarchical clustering was performed using Euclidean distance and the complete linkages method. For heatmap/cluster analysis, fold change data were calculated relative to the wild-type Col-0 at LL and log2 scaled. A heatmap was then generated using the heatmap.2 package in R software, using the Euclidean distance algorithm for dendrogram creation. The dendrogram was cut into 6 clusters.

Metabolic Modelling

We used a metabolic model modified from that of Arnold and Nikoloski (2014), as previously published

Posted on Authorea 21 Jul 2020 — The copyright holder is the author/funder. All rights reserved. No reuse without permission. — https://doi.org/10.22541/au.159534893.31472268 — This a preprint and has not been peer reviewed. Data may be preliminary.

(Herrmann, Dyson, Vass, Johnson, & Schwartz, 2019). Specifically, the model was modified to ensure that cytosolic fumarate could be produced from cytosolic malate (inclusion of reversible cytosolic FUM reaction) and added "export reactions" to the model (describing diurnal storage pools) for malate, fumarate and starch, in addition to the already existing sucrose export. Additionally, we added a cyclic electron transport reaction to the model which was previously missing. We generated four models for each genotype (Col-0 and *fum2*): 20°C; 4°C on Day 0; 4°C on Day 7 of treatment; and one with NADPH-limiting conditions. We constrained the models using metabolite assays such that the beginning-of-day concentrations of fumarate, malate, and starch subtracted from their respective end-of-day concentrations equated to the diurnal flux over the eight-hour photoperiod, consistent with an approximately constant rate of accumulation of these metabolites seen experimentally (Dyson *et al.* , 2016). We assumed a constant rate of photosynthesis through the day (Dyson *et al.* , 2016) and converted the measured rates of photosynthesis to cumulative diurnal fluxes of carbon intake ($mmol.gFW^{-1}.Day^{-1}$), as previously described by Herrmann *et al.* (2019) . Flux to sucrose was not constrained but was used to estimate the remaining carbon which is exported from the leaf during the day. We then used proteomics data to further constrain the upper bounds of the flux reactions (Ramon, Gollub, & Stelling, 2018). For each metabolic reaction we checked whether all of the corresponding proteins were available in the data set; if so, then those reactions were given an upper bound of the additive values of all of the identified proteins, in case multiple isoforms exist. The proteomic constraints of the Col-0 and *fum2*20°C models we also applied to the respective 4°C Day 0 models, assuming that during the first day of cold, changes in metabolic enzyme content are negligible (consistent with measured total protein and photosynthetic capacity). Given that the proteomics data are relative and not quantitative, we scaled all the proteomics constraints to the lowest possible values for which we were able to obtain model solutions across all models. In total, we constrained the upper bounds of 101 reactions in each model. Proteomic constraints were calculated as the averages of four biological replicates for each treatment plus the standard error of those measurements, thus accounting for measurement error. Because protein presence does not necessarily equate to enzymatic activity, we set the lower bounds for these reactions to zero for irreversible reactions and to the negative value of the upper bound for reversible reactions. Proteomic constraints were applied only to the "inner" model reactions, whereas the metabolite and photosynthesis data were used to set boundary conditions (i.e. influxes and effluxes). We the used flux solutions, from a flux balance analysis maximizing carbon assimilation via Rubisco within feasible model constraints, in order to eliminate non-essential reactions which generate loops within the model, using the loopless function in the *cobra* (version 0.10.1) package (Desouki, Jarre, Gelius-Dietrich, & Lercher, 2015). The objective function is irrelevant to the results presented in this paper and was only applied to ensure that none of the pathways required for carbon metabolism contained thermodynamically infeasible solutions. We then conducted flux sampling on the loopless models using the CHRR algorithm in the MATLAB toolbox as outlined in Herrmann *et al.* (2019). In order to minimise observer bias, the flux sampling was performed without an optimisation constraint for the control, Day 0 and Day 7 models. The NADPH-limited models are the same as the control models, but here, in addition to the experimental constraints, we set a minimum NADPH production via linear electron transport as an objective function.

Network Analysis

We converted the metabolic model to a metabolite-metabolite graph of primary carbon metabolism using the method of Ranganathan and Maranas (2010). A full list of the nodes and edges is available on Zenodo (DOI: 10.5281/zenodo.3366934). We then used the networkx (version 1.10) package in Python (Version 3.6.9) in order to iteratively identify pathways with fewer than 20 nodes connecting Rubisco and fumarate node. We checked the 17 identified pathways against the flux sampling solutions of the Col-0 models and identified two pathways which carried a flux substantial enough to account for fumarate accumulation in the model. All other pathways had at least one reaction for which the sampling solutions were either zero or close to zero. For fluxes to be considered close to zero, we used a cut-off of 0.4, which is 3 times lower than the carbon flux to fumarate (i.e. not substantial enough to explain our observed accumulation of fumarate in wild-type Col-0 plants).

Data Availability

Posted on Authorea 21 Jul 2020 — The copyright holder is the author/funder. All rights reserved. No reuse without permission. — https://doi.org/10.22541/au.159534893.31472268 — This a preprint and has not been peer reviewed. Data may be preliminary.

All models, code and data used to conduct the computational analyses are available at https://github.com/HAHerrmann/FluxSamplingCol0Fum2 and have been archived in Zenodo (DOI: 10.5281/zenodo.3366934).

Results

Acclimation of both photosynthesis and respiration to cold are impaired in plants lacking FUM2

Plants of the wild-type Arabidopsis, accession Col-0 and a mutant in the same background, *fum2.2* , were grown for 8 weeks at a daytime temperature of 20°C. Plants were then transferred to a growth cabinet with the same light conditions, but with a temperature of 4°C. Photosynthetic capacity (P_{max}; measured at 20°C in saturating light and CO_2) of these plants was measured over the following 9 days (Figure 1 a). Prior to transfer to low temperature, P_{max} of Col-0 was slightly higher than that of *fum2.2* . Following one day at low temperature, the capacity for photosynthesis (P_{max}) in Col-0 increased. P_{max} continued to increase over the following days, rising to a new steady state approximately 50% higher than the starting value by the sixth day of cold treatment. This indicates that, under our experimental conditions, dynamic acclimation of photosynthesis occurs in response to cold and that a new steady-state is reached within 7 days. In contrast, the P_{max} of *fum2.2* did not vary over the course of the experiment, confirming previous evidence that both*fum2.1* and *fum2.2* mutants lacking FUM2 are unable to acclimate their photosynthetic capacity in response to cold (Dyson*et al.* , 2016).

Measurements of the rate of gas exchange achieved by plants in growth cabinets, with ambient CO_2, light and temperature, were performed in the last hour of the first day of cold. Transfer to cold resulted in a small but significant inhibition of both photosynthesis and respiration at the end of the first day of exposure to cold (ANOVA, $P<0.05$; Figure 1 b,c). In Col-0, acclimation of both parameters had occurred after 7 days, such that *in situ* rates of gas exchange recovered and did not differ significantly from those recorded at 20°C prior to acclimation. In contrast, in *fum2.2* , no recovery occurred in either photosynthesis or respiration. This suggests that either fumarate accumulation or FUM2 protein, is essential for the acclimation of both photosynthesis and respiration to cold.

Acclimation to cold changes partitioning of metabolites between sinks

In plants, diurnally-produced organic carbon can be directly exported from the leaf, used in cellular respiration, or stored in the leaf in a variety of forms (Chia, Yoder, Reiter, & Gibson, 2000; Fahnenstich*et al.* , 2007; Zell *et al.* , 2010). In Arabidopsis, the principal leaf carbon stores are starch and organic acids, especially fumarate and malate (Chia *et al.* , 2000; Zell *et al.* , 2010). When plants are exposed to cold for a single photoperiod, the accumulation of both starch and organic acids increases (Dyson *et al.* , 2016). Here, we measured the beginning and end of photoperiod concentrations of starch, fumarate and malate in Col-0 and *fum2.2* on each of the 7 days following transfer to cold (Figure 2). The diurnal accumulation of these metabolites shows clear evidence of acclimation in both genotypes. In both wild-type Col-0 and *fum2.2* , starch accumulation was greater at 4°C than 20°C on the first day of cold and increased each day, until Day 4 of cold treatment (Figure 2 a). The amount of starch seen at the end-of-day was higher in*fum2.2* than in Col-0 throughout the experiment, with the absolute difference between genotypes remaining approximately constant throughout the treatment. In Col-0, essentially all starch accumulated during the day was mobilised overnight throughout the acclimation period. In*fum2.2* , a small amount of starch was retained in the leaf at dawn after the third day of cold treatment.

In Col-0, there was an increase in the amount of fumarate accumulated each day through the acclimation period (Figure 2 b). This was accompanied by an increase in the accumulation of malate (Figure 2 c), such that these acids represented an increased proportion of total stored carbon. In *fum2.2* , the amount of fumarate was always substantially lower than in Col-0 and at no point in the experiment was there evidence of a diurnal accumulation of fumarate. End-of-day malate concentrations were increased on the first day of cold in *fum2.2*but then fell the following day, before rising again towards the end of the treatment period.

Posted on Authorea 21 Jul 2020 — The copyright holder is the author/funder. All rights reserved. No reuse without permission. — https://doi.org/10.22541/au.159534893.31472268 — This a preprint and has not been peer reviewed. Data may be preliminary.

Arabidopsis does not accumulate substantial amounts of sucrose in its leaves under most conditions, but sucrose is known to play an important role in freezing tolerance (Stitt & Hurry, 2002). We assayed leaf sucrose and glucose content in response to cold treatment (Figure S1). At 20°C, there is a significant diel cycle in sucrose content, however, in response to cold treatment, this cycle was lost in both genotypes, with beginning-of-day sucrose content increasing and end-of-day content decreasing progressively through the week. At the end of the cold treatment, *fum2.2* contained slightly more sucrose than wild-type Col-0.

To understand better how carbon is partitioned between different diurnal storage pools in different conditions, we combined data from Figures 1-2, S1 and from Dyson*et al.* (2016) to perform a carbon budget audit (Figure 3). The accumulation of starch, sucrose, fumarate and malate were estimated as the difference in beginning- and end-of-day concentrations (Figure 2, S1). Rates of gas exchange were measured under growth conditions at intervals through the photoperiod (See Figure 1c and Dyson *et al.* , 2016) and were used to calculate the daily carbon uptake and respiratory consumption. The difference between carbon fixed through photosynthesis and the measured carbon fluxes to respiration and known carbon stores was assumed to be largely accounted for by carbon export from the leaf in the form of sucrose, consistent with estimates from Lundmark, Cavaco, Trevanion, and Hurry (2006), although other compounds may accumulate or be exported from the leaf and are included in this category.

Plants of *fum2.2* at 20°C showed similar photosynthesis and respiration to Col-0. Although they do not accumulate fumarate, the proportion of total carbon stored as organic acid was similar to that seen in Col-0, with an increased accumulation of malate. Combining this with the increase in starch accumulation, which is larger in*fum2.2* than in Col-0 we conclude that the total unaccounted carbon, primarily diurnal export, is lower in *fum2.2* than in Col-0.

During the first day of exposure to cold, there were notable changes in carbon distribution between different sinks (Figure 3 a, b). Total fixed carbon was lower on Day 0 (first day) of cold due to the lower rate of photosynthesis (Figure 1). In both genotypes, the total amount of fixed carbon we were able to account for increased, implying that diurnal carbon export is probably inhibited. Unaccounted carbon was still greater in Col-0 than in *fum2.2* . When plants were cold-treated for 7 days, this effect became even more marked (Figure 3 d). From this, we conclude that there is a substantial inhibition of diurnal carbon export from the leaf in cold treated plants of both genotypes, but that this effect becomes more pronounced in *fum2.2* over the course of the week. Given that all metabolite pools retain a diel turnover, we conclude that metabolic acclimation to cold involves a shift from diurnal carbon export to nocturnal processes.

Acclimation to cold involves changes in the proteome of both Col-0 and fum2.2

In a previous study of dynamic acclimation, we saw that photosynthetic acclimation to increased light entails an increase in enzyme concentrations involved in multiple metabolic processes (Miller *et al.* , 2017). In Col-0, cold exposure for 7 days resulted in a significant increase in leaf protein content (Figure 4 a), with an approximately 30% increase in protein content per unit fresh weight of leaf. In *fum2.2* , protein content did not change significantly. Nevertheless, analysis of the proteome shows that there were changes occurring in both Col-0 and*fum2.2* , albeit to a much smaller extent in the latter. We were able to estimate the relative abundance of 2427 polypeptides, based on a minimum of 3 unique peptides per protein. Principal Component Analysis of proteomic data indicates that the proteomes of Col-0 and*fum2.2* differ already under 20°C conditions, however there is a clear separation of cold treated plants from their corresponding 20°C controls in both genotypes (Figure 4 b). Cluster analysis was performed using data from the 2015 proteins which showed significantly altered expression in one of more conditions. As expected, given the total increase in protein, the most common response to cold is for proteins to increase in Col-0 but less so or not at all in *fum2.2* (Figure 4 c,d,g). A far smaller cluster of proteins increased in both genotypes following cold treatment (Figure 4 e) whilst a few proteins decreased in response to cold in *fum2.2*(Figure 4 f).

Examination of the relative concentration of proteins involved in the photosynthetic electron transport chain demonstrated that only subtle changes were occurring (Table S1). There were increases in the relative abundance of various peripheral PSII proteins, including isoforms of PSBS, and in PSB29, which has been

Posted on Authorea 21 Jul 2020 — The copyright holder is the author/funder. All rights reserved. No reuse without permission. — https://doi.org/10.22541/au.159534893.31472268 — This a preprint and has not been peer reviewed. Data may be preliminary.

implicated in PSII assembly (Keren*et al.* , 2005), however components of the PSII core did not change significantly in response to cold. Amongst the proteins of the photosynthetic electron transport chain, 2 of the 4 detected cytochrome b6f complex subunits increased significantly in Col-0; measurements for the other subunit were too variable to allow a confident assessment of changes in abundance. Overall, this suggests a tendency to increase cytochrome b_6f abundance in Col-0, whilst in*fum2.2* there is no evidence for a change in the abundance of this complex. While plastocyanin showed no change in abundance in either genotype, the only detected ferredoxin isoform increased in both genotypes, as did one of the four detected FNR isoforms. 4 of the detected 8 ATP synthase subunits were upregulated in Col-0, whilst 2 showed a significant change in *fum2.2* . Taking these data overall, we conclude that there were no changes in photosystem stoichiometry in response to cold in either genotype and that changes in electron transport proteins in Col-0 were either reduced or absent in*fum2.2* . There were however consistent and significant differences between the genotypes both in warm and cold conditions, with a greater abundance of subunits of all complexes seen in Col-0.

In contrast to the components of the photosynthetic electron transport chain, changes in the enzymes associated with the Benson Calvin cycle gave a clearer and more consistent pattern of response (Figure 5). The CO_2 fixing enzyme, Rubisco, is by far the most abundant protein in the leaf. We were able to quantify the chloroplast-encoded large subunit (RBCL) and 2 isoforms of the nuclear-encoded small subunit, RBCS. All increased significantly in Col-0 in response to cold, with a mean 1.8-fold increase in relative abundance. In *fum2.2*there was no significant change in RBCL abundance. One isoform of RBCS increased significantly, whilst the other decreased to a similar extent. Combining data from both isoforms, there was no significant change in RBCS abundance. For other reactions associated with the Benson Calvin cycle, we were able to quantify a total of 20 distinct proteins, including isoforms of specific enzymes. In Col-0, 14 of these significantly increase, whilst 5 decreased. In *fum2.2* , although 6 enzymes involved in the Benson Calvin cycle came out as significantly increased, the overall extent of this change was lower.

Across other major metabolic pathways – including starch and sucrose synthesis, glycolysis and the tricarboxylic acid cycle, similar patterns of acclimation were observed, with most proteins increasing in the cold in Col-0 and *fum2.2* but to a lesser extent in the latter case (Table S1). In the sucrose synthesis pathway, most enzymes increased their concentration in response to cold in both genotypes, but with the relative abundance of these tending to be lower in *fum2.2* (Figure S2). A notable exception to this was sucrose phosphate phosphatase, which did not increase in *fum2.2* .

To summarise, acclimation of photosynthesis to low temperature in Col-0 involves an increase in the abundance of some electron transfer proteins, though not reaction centres, and substantial changes in the amount of a broad range of Benson Calvin cycle enzymes, consistent with increases seen in enzyme activities in response to cold observed previously (Strand *et al.* , 1999). These changes are largely or completely absent in *fum2.2* . Changes in the proteome across metabolism show a similar tendency but to a different extent in other metabolic pathways. These data indicate that fumarate accumulation or FUM2 protein or activity plays a central role in high-level processes regulating acclimation of a wide range of metabolic enzymes.

Metabolic modelling shows that cold induces an alteration in carbon export from the chloroplast which is perturbed in

fum2.2

Results presented here show that acclimation to cold results in a substantial change in the metabolism of Col-0 plants, with a shift from diurnal to nocturnal carbon export from the leaf and an increase in leaf diurnal carbon storage. In *fum2.2* a similar shift occurs, but with a different distribution of carbon between pools. Plants of*fum2.2* carry out significantly less photosynthesis in the cold but retain a greater proportion of fixed carbon in the leaf. Although the protein changes in *fum2.2* are less marked than in Col-0, there is nevertheless evidence of metabolic changes over the week. To better understand the factors underlying these changes in the two genotypes, we adopted a modelling approach.

Modelling was performed using flux sampling (Herrmann *et al.* , 2019) based on a modified version of the model of Arnold and Nikoloski (2014; see Methods for details). We set up metabolic models for the Col-

Posted on Authorea 21 Jul 2020 — The copyright holder is the author/funder. All rights reserved. No reuse without permission. — https://doi.org/10.22541/au.159534893.31472268 — This a preprint and has not been peer reviewed. Data may be preliminary.

0 and *fum2* genotypes and constrained them using experimental data to represent possible flux solutions under control conditions and on the 1st and 7th days of cold treatment. Constraining the model using the proteomic data allowed us to analyse the above observed difference in Col-0 and *fum2* plants in response to cold, including changes in the electron transport proteins and Benson Calvin cycle enzymes, in a system context.

In order to determine feasible pathways by which assimilated carbon can be converted to cytosolic fumarate, we validated potential pathways against the flux sampling results as outlined in the Materials and Methods in order to see whether they were carrying a significant flux under the given model constraints. The flux sampling results confirmed two of these pathways to be feasible in the Col-0 and *fum2*20°C models (Figure 6). These pathways differ from one another in terms of their relative consumption of ATP and NADPH. Activity of Rubisco produces 3-phosphoglyceric acid (PGA) from ribulose-1.5-phosphate and CO_2. PGA can then be converted to triose phosphate (TP) in reactions requiring ATP and NADPH. There are two forms of TP (glyceraldehyde-3-phosphate and dihydroxy acetone phosphate); when exporting either of the two forms from the chloroplast in our analysis we obtained the same results and therefore refer to the two forms collectively as TP export. TP is exported from the chloroplast in exchange for inorganic phosphate by the triose phosphate translocator (TPT). Conversion of TP to fumarate includes the reconversion of TP to PGA in the cytosol. The PGA is then carboxylated and reduced to form malate. The TPT is also capable of exporting PGA directly, eliminating the reduction reaction in the chloroplast.

Our flux sampling results highlight that the export of PGA versus TP from the chloroplast varies under changing conditions using flux sampling (Figure 7). In models of 20°C conditions, most carbon is exported from the chloroplast in the form of TP, with the*fum2* model tending to have higher PGA export (Figure 7 a,e). In the Day 0 cold model, where the rate of photosynthesis is restricted, PGA export is increased and TP export is decreased in Col-0, whilst in*fum2* both show a tendency to be reduced (Figure 7 b,f). In Col-0 plants acclimated to cold ("Day 7 – 4°C"), where the rate of photosynthesis recovers (Figure 1 b), PGA export is modelled to decrease relative to Day 0, while TP export is largely unaffected (Figure 7 c,g). At the same time, in the *fum2* model, which does not consider a recovery of the photosynthetic rate (Figure 1 b). PGA export it largely absent.

Previous experimental data have indicated that the ATP/NADPH ratio increases at low temperature in Arabidopsis (Savitch *et al.* , 2001), possibly reflecting changes in the ratio of cyclic to linear electron transport (Clarke & Johnson, 2001). To simulate this, we ran the Col-0 and *fum2* 20°C models with their NADPH production restricted (simulating a restriction in electron transport capacity). When limiting the NADPH production in the cell (by setting minimum NADPH production as an optimisation constraint) similar effects to the initial cold response in Col-0 and *fum2* were achieved (Figure 7 d,h). Again, PGA export increased in Col-0, this time even more markedly than in response to cold. By implementing cyclic electron flow in the model, it makes sense that a reduced rate of photosynthesis on the first day of photosynthesis will have a similar effect to limiting NADPH production. Whilst metabolic modelling suggests an increase in PGA:TP export from the chloroplast under cold and NADPH-limited conditions, this effect is not observed in the *fum2*models. In fact, for *fum2,* PGA export is potentially highest in 20°C conditions (Figure 7 a).

One week of cold treatment affects the seed production of*fum2.2* plants

Arabidopsis Col-0 and *fum2.2* plants grown in control conditions and plants that received one week of cold treatment after 8 weeks growth, were transferred into a growth cabinet with a 16-hour photoperiod to induced flowering. Plants were allowed to set seed and seed yield estimated (Figure 8). No significant difference was seen between the seed yield of Col-0 plants maintained at 20°C and those that experienced a cold treatment. In contrast, when *fum2.2* plants were exposed to cold for 7 days before being transferred to long photoperiods, the final seed yield was significantly reduced. This reduction was due to a lower number of siliques being formed, rather than a reduction in the number of seeds per silique.

Discussion

Previous work has shown that the ability to acclimate photosynthesis and metabolism to changes in light

Posted on Authorea 21 Jul 2020 — The copyright holder is the author/funder. All rights reserved. No reuse without permission. — https://doi.org/10.22541/au.159534893.31472268 — This a preprint and has not been peer reviewed. Data may be preliminary.

plays an important role in determining plant fitness and seed yield (Athanasiou*et al.* , 2010). Here, we have presented evidence that acclimation to cold is also important in determining fitness and seed yield - wild-type Col-0 plants are unaffected by changes in temperature, while*fum2.2* , which is unable to acclimate to cold, is negatively affected by even short cold periods. Ability to acclimate photosynthesis to environmental change is therefore clearly an important process that will have major impacts on crop yields and may be a target for crop breeding.

Previously, we have seen that acclimation of photosynthetic capacity to both light and temperature involves metabolic signalling, as evidenced by knockouts of either the glucose-6-phosphate/phosphate translocator GPT2 or of the cytosolic fumarase FUM2 being deficient in their acclimation responses (Athanasiou*et al.* , 2010; Dyson *et al.* , 2015; Dyson *et al.* , 2016; Miller *et al.* , 2017). Recently, Weise *et al.* (2019) confirmed that the increase in GTP2 transcripts in response to environmental change is linked to TPT export and that this link is an important feature of day-time metabolism. Here we show that cold acclimation involves a reconfiguration of diel carbon metabolism of the leaf, with a major shift in the ratio of diurnal carbon leaf storage to export. Plants acclimated to cold retain more carbon in the leaf during the day and therefore must export more overnight. Furthermore, we provide evidence from metabolic modelling that acclimation responses may depend on the form of carbon export from the chloroplast. Specifically, we propose that the PGA:TP chloroplast export ratio provides a novel potential signal, which may drive aspects of acclimation responses both in the chloroplast and the wider cell.

Earlier studies on the cold acclimation of photosynthesis in Arabidopsis highlighted the importance of sucrose synthesis and, specifically, the activity of sucrose phosphate synthase (Stitt & Hurry, 2002; Strand, Foyer, Gustafsson, Gardestrom, & Hurry, 2003). It was suggested that phosphate recycling is impaired at low temperature, due to the accumulation of sugar phosphates, such as glucose-6-phosphate, fructose-1.6.-bisphosphate and fructose-6-phosphate. Evidence from the*fum2.2* mutant speaks against a direct role for phosphate in controlling the acclimation of photosynthetic capacity. Non-acclimating*fum2.2* plants show higher levels of sugar phosphates on the first day of cold than do Col-0 plants, and should therefore have a stronger photosynthetic acclimation signal (Dyson *et al.* , 2016). If phosphate is a signal for acclimation, fumarate accumulation must play a role down-stream of this, preventing acclimation despite the signal. This conclusion is further supported here. Measurements of the major sugar phosphates involved in sucrose synthesis (Figure S2) shows that these tend to increase as a result of acclimation. There is however no persistent significant difference in the concentrations of these in the different genotypes. Phosphate may still play a role in the short-term regulatory responses seen on exposure to cold (Hurry *et al.* , 2000).

Regardless of the role of phosphate in cold sensing, diurnal flux to sucrose is clearly an important part of the cold response. On the first day of exposure to cold, the estimated maximum possible flux to sugar export dropped significantly, compared to plants maintained at 20°C (Figure 3 c,d). This effect might be explained by a drop in sink strength, however, if this is the case, then it is not alleviated by acclimation at the whole plant level. If the reduction in daytime export is indeed sink limited, it is unlikely to be a consequence of the overall capacity of sinks since, over the diel cycle, there was no evidence of progressive accumulation of fixed carbon in the leaf. Thus, nocturnal processes, including export from the leaf or increased nocturnal respiration, compensate for diurnal export.

Nocturnal metabolism of leaves remains poorly understood. At night, there is a highly controlled mobilisation of starch, which is maintained at an approximately constant rate through the night (Graf & Smith, 2011; Smith & Stitt, 2007). It has also been shown that organic acids (malate and fumarate) make an important contribution to nocturnal metabolism – plants with reduced organic acid storage due to over-expression of plastidic malate dehydrogenase, are less fit under short day growth conditions and show a carbon starvation response, metabolising fatty acids and proteins to replace organic acids (Zell*et al.* , 2010). Our data show that stored organic acids are also mobilised overnight both under warm and cold conditions (Dyson *et al.* , 2016). Carbon export in Arabidopsis is thought to largely be in the form of sucrose, however it is not clear in detail how this is synthesised, either from starch or organic acids. Starch breakdown involves the formation of maltose (di-glucose) and glucose molecules, which are exported from the chloroplast. If synthesis

Posted on Authorea 21 Jul 2020 — The copyright holder is the author/funder. All rights reserved. No reuse without permission. — https://doi.org/10.22541/au.159534893.31472268 — This a preprint and has not been peer reviewed. Data may be preliminary.

of sucrose follows the same pathway as in the daytime, the glucose would need to be phosphorylated, by hexokinase, before being incorporated into sucrose. Sucrose phosphate synthase (SPS) is the major enzyme responsible for the diurnal synthesis of sucrose (Huber & Huber, 1996). It is not clear why this pathway would operate more efficiently at night than it does during the day. It may therefore be that an alternative pathway for sucrose synthesis at night exists. We did observe a substantial increase in the concentration of the main isoform of sucrose synthase (SS) following cold acclimation (Table S1). SS produces sucrose from the reaction of UDP-glucose with fructose, in contrast to SPS which reacts UDP-glucose with fructose-6-phosphate (Stein & Granot, 2019). SS would in theory represent a lower energy pathway to generate sucrose from hexoses. However, SS is generally believed to operate in the direction of sucrose breakdown, releasing glucose for metabolic processes. It is therefore not obvious why SS would normally be present in mature leaves, which are net sources for carbon, and which do not store sucrose to a significant degree. It is possible though that night-time sucrose synthesis may involve SS.

The synthesis of fumarate has an impact on diurnal carbon export from the leaf which cannot be explained by a reduction in storage capacity. At 20°C, *fum2.2* plants maintain a similar photosynthetic rate but store a larger proportion of total carbon in the leaf than do wild-type Col-0 plants. Although fumarate accumulation is inhibited, this is largely compensated for by increased accumulation of malate. At the same time, starch storage is also greater. As in Col-0, short term exposure to cold increases this effect and following 7 days acclimation, only a very small proportion of fixed carbon is exported during the day.

The role of fumarate accumulation in Arabidopsis leaves is not, we conclude, a simple carbon sink effect; it is affecting the overall distribution of carbon between different storage pools in ways that cannot simply be explained by a loss of storage capacity. In order to better understand the possible processes affected by fumarate accumulation, we adopted a modelling approach. Using a network analysis of a metabolite-metabolite graph, we identified several potential pathways for fumarate synthesis. When modelling potential flux solutions for these pathways, only two of the identified pathways carried a significant flux. These involve export of fixed carbon from the chloroplast in the form of either phosphoglyceric acid (PGA) or triose phosphate (TP – glyceraldehyde-3-phosphate and dihydroxy acetone phosphate). These compounds are all transported by the same translocator – the triose phosphate translocator (TPT) – which is reported to have very similar transport properties for these different compounds (Knappe, Flugge, & Fischer, 2003). A comparison of plants lacking one or the other of these exports is therefore not possible via traditional experimental approaches such as reverse genetics or using inhibitors.

Here we have applied flux sampling (Herrmann *et al.* , 2019) to gain an understanding of the impact of fumarate synthesis on wider metabolism. Flux sampling is a novel constraint-based modelling approach that has the advantage over flux balance analysis and flux variability analysis that the entire solution space can be captured in the form of a frequency distribution and hence it allows for a more precise comparison of different sets of constraints (Herrmann *et al.* , 2019). Building on a published model (Arnold & Nikoloski, 2014), we show that export of carbon from the chloroplast can occur either as PGA or TP. The model was constrained using experimental data: carbon input and fluxes to major storage sinks were set according to measured physiological parameters, and the relative capacity of individual reactions were constrained in proportion to changes in the proteome (Table S1). The broad validity of this model comes from the observation that carbon export from the leaf, which was not constrained, varied in a way that is consistent with the experimental data (Figure 3 c,d, Figure S3). Based on this, we conclude that an increase in the proportion of carbon exported as PGA is an initial response to cold in Col-0 plants. Furthermore, we were able to demonstrate that, in the Col-0 model, the ratio of PGA:TP export varies as a function of NADPH supply from the photosynthetic electron transport chain. Limitation in NADPH is known to be an early response to low temperature, as flux through the linear electron transport chain decreases (Clarke & Johnson, 2000). At the same time, cyclic electron flow at low temperature will tend to increase the ATP:NADPH ratio. NADPH in the chloroplast is essential for the conversion of PGA into TP. Limited NADPH supply will tend to favour PGA export. Thus, the relative export of PGA and TP from the chloroplast encodes information about the redox state of the chloroplast and as a result has the potential to act as a signal to the nucleus controlling acclimation to changing conditions.

Posted on Authorea 21 Jul 2020 — The copyright holder is the author/funder. All rights reserved. No reuse without permission. — https://doi.org/10.22541/au.159534893.31472268 — This a preprint and has not been peer reviewed. Data may be preliminary.

PGA in the cytosol is converted to phosphoenolpyruvate (PEP) and then carboxylated by PEP carboxylase for form oxaloacetate (OAA). OAA is in turn reduced by malate dehydrogenase to form malate. In our modelling, the net accumulation of malate and fumarate was constrained to experimental levels, nevertheless, it remains unclear why flux to malate would be biologically different to flux to fumarate, given that these acids exist in equilibrium, catalysed by fumarase. One possible explanation though lies in the regulation of PEP carboxylase, which is subject to feedback inhibition by malate (Wedding, Black, & Meyer, 1990). If malate accumulates, this is liable to feedback to inhibit its own synthesis. Removing malate, converting it to fumarate, ensures that this pathway does not become limiting. This may be essential to ensure that fluxes away from PGA are not sink limited, so ensuring the PGA concentrations in the cytosol reflect the rate of export and do not accumulate over the photoperiod.

In conclusion, we have shown that the ability to accumulate fumarate in Arabidopsis leaves has wide-ranging impacts on diurnal carbon partitioning in the leaf. Lack of fumarate synthesis results in widespread differences being seen across the proteome and prevents the acclimation of photosynthetic capacity to low temperature. Fumarate accumulation is important in facilitating diurnal carbon export from the leaf. Low temperatures inhibit diurnal sucrose export and this effect is exacerbated in plants lacking fumarate accumulation. Modelling of leaf metabolism suggests that the relative export of PGA and TP may be an important signal reflecting the redox poise of the chloroplast. As such it has the potential to act as a signal controlling the expression of nuclear genes which underlies photosynthetic acclimation to environmental change.

Acknowledgements: We would like to thank Drs David Knight, Ronan O'Cualain and Julian Selley (University of Manchester) for their help with the proteomic analysis. This work was supported by a grant from the Biotechnology and Biological Sciences Research Council (BBSRC; BB/J04103/1). HAH and MAEM were supported BBSRC studentships (BB/M011208/1).

References

Armstrong, A. F., Logan, D. C., Tobin, A. K., O'Toole, P., & Atkin, O. K. (2006). Heterogeneity of plant mitochondrial responses underpinning respiratory acclimation to the cold in Arabidopsis thaliana leaves. *Plant, Cell & Environment, 29* (5), 940-949. doi:10.1111/j.1365-3040.2005.01475.x

Arnold, A., & Nikoloski, Z. (2014). Bottom-up Metabolic Reconstruction of Arabidopsis and Its Application to Determining the Metabolic Costs of Enzyme Production. *Plant Physiology, 165* (3), 1380-1391. doi:10.1104/pp.114.235358

Athanasiou, K., Dyson, B. C., Webster, R. E., & Johnson, G. N. (2010). Dynamic acclimation of photosynthesis increases plant fitness in changing environments. *Plant Physiology, 152* , 366-373. doi:http://www.plantphysiol.org/cgi/reprint/152/1/366

Chia, D. W., Yoder, T. J., Reiter, W. D., & Gibson, S. I. (2000). Fumaric acid: an overlooked form of fixed carbon in Arabidopsis and other plant species. *Planta, 211* (5), 743-751.

Clarke, J. E., & Johnson, G. N. (2000). In vivo temperature dependence of cyclic and pseudocyclic electron transport in barley. *Planta* .

Desouki, A. A., Jarre, F., Gelius-Dietrich, G., & Lercher, M. J. (2015). CycleFreeFlux: efficient removal of thermodynamically infeasible loops from flux distributions. *Bioinformatics, 31* (13), 2159-2165. doi:10.1093/bioinformatics/btv096

Dyson, B. C., Allwood, J. W., Feil, R., Xu, Y. U. N., Miller, M., Bowsher, C. G., . . . Johnson, G. N. (2015). Acclimation of metabolism to light in Arabidopsis thaliana: the glucose 6-phosphate/phosphate translocator GPT2 directs metabolic acclimation. *Plant, Cell & Environment, 38* (7), 1404-1417. doi:10.1111/pce.12495

Dyson, B. C., Miller, M. A. E., Feil, R., Rattray, N., Bowsher, C. G., Goodacre, R., . . . Johnson, G. N. (2016). FUM2, a Cytosolic Fumarase, Is Essential for Acclimation to Low Temperature in <em>Arabidopsis thaliana</em&gt. *Plant Physiology, 172* (1), 118-127.

Posted on Authorea 21 Jul 2020 — The copyright holder is the author/funder. All rights reserved. No reuse without permission. — https://doi.org/10.22541/au.159534893.31472268 — This a preprint and has not been peer reviewed. Data may be preliminary.

Fahnenstich, H., Saigo, M., Niessen, M., Zanor, M. I., Andreo, C. S., Fernie, A. R., . . . Maurino, V. G. (2007). Alteration of organic acid metabolism in Arabidopsis overexpressing the maize C(4)NADP-malic enzyme causes accelerated senescence during extended darkness. *Plant Physiology, 145* (3), 640-652. doi:10.1104/pp.107.104455

Fey, V., Wagner, R., Brautigam, K., & Pfannschmidt, T. (2005, 2005).*Photosynthetic redox control of nuclear gene expression.* Paper presented at the International Botanical Congress, Vienna, AUSTRIA.

Graf, A., & Smith, A. M. (2011). Starch and the clock: the dark side of plant productivity. *Trends in Plant Science, 16* (3), 169-175. doi:10.1016/j.tplants.2010.12.003

Herrmann, H. A., Dyson, B. C., Vass, L., Johnson, G. N., & Schwartz, J.-M. (2019). Flux sampling is a powerful tool to study metabolism under changing environmental conditions. *npj Systems Biology and Applications, 5* (1), 32. doi:10.1038/s41540-019-0109-0

Huber, S. C., & Huber, J. L. (1996). Role and regulation of sucrose-phosphate synthase in higher plants. *Annual Review of Plant Physiology and Plant Molecular Biology, 47* , 431-444. doi:10.1146/annurev.arplant.47.1.431

Huner, N. P. A., Öquist, G., Hurry, V. M., Krol, K., Falk, S., & Griffith, M. (1993). Photosynthesis, photoinhibition and low temperature acclimation in cold-tolerant plants. *Photosynthesis Research, 37* , 19-39.

Hurry, V., Strand, Å., Furbank, R., & Stitt, M. (2000). The role of inorganic phosphate in the development of freezing tolerance and the acclimatization of photosynthesis to low temperature is revealed by the pho mutants of Arabidopsis thaliana. *The Plant Journal, 24* (3), 383-396. doi:10.1046/j.1365-313x.2000.00888.x

Knappe, S., Flugge, U. I., & Fischer, K. (2003). Analysis of the plastidic phosphate translocator gene family in Arabidopsis and identification of new phosphate translocator-homologous transporters, classified by their putative substrate-binding site. *Plant Physiology, 131* (3), 1178-1190.

Knight, M. R., & Knight, H. (2012). Low-temperature perception leading to gene expression and cold tolerance in higher plants. *New Phytologist, 195* (4), 737-751.

Lundmark, M., Cavaco, A. M., Trevanion, S., & Hurry, V. (2006). Carbon partitioning and export in transgenic Arabidopsis thaliana with altered capacity for sucrose synthesis grown at low temperature: a role for metabolite transporters. *Plant Cell and Environment, 29* (9), 1703-1714. doi:10.1111/j.1365-3040.2006.01543.x

Miller, M. A. E., O'Cualain, R., Selley, J., Knight, D., Karim, M. F., Hubbard, S. J., & Johnson, G. N. (2017). Dynamic Acclimation to High Light in Arabidopsis thaliana Involves Widespread Reengineering of the Leaf Proteome. *Frontiers in plant science, 8* , 1239. doi:10.3389/fpls.2017.01239

Pracharoenwattana, I., Zhou, W. X., Keech, O., Francisco, P. B., Udomchalothorn, T., Tschoep, H., . . . Smith, S. M. (2010). Arabidopsis has a cytosolic fumarase required for the massive allocation of photosynthate into fumaric acid and for rapid plant growth on high nitrogen. *Plant Journal, 62* (5), 785-795. doi:10.1111/j.1365-313X.2010.04189.x

Ramon, C., Gollub, M. G., & Stelling, J. (2018). Integrating -omics data into genome-scale metabolic network models: principles and challenges. *Essays in Biochemistry, 62* (4), 563-574. doi:10.1042/ebc20180011

Ranganathan, S., & Maranas, C. D. (2010). Microbial 1-butanol production: Identification of non-native production routes and in silico engineering interventions. *Biotechnol J, 5* (7), 716-725. doi:10.1002/biot.201000171

Ruelland, E., Vaultier, M.-N., Zachowski, A., & Hurry, V. (2009). Cold Signalling and Cold Acclimation in Plants. In J. C. Kader & M. Delseny (Eds.), *Advances in Botanical Research, Vol 49* (Vol. 49, pp. 35-150).

Savitch, L. V., Barker-Astrom, J., Ivanov, A. G., Hurry, V., Oquist, G., Huner, N. P. A., & Gardestrom, P. (2001). Cold acclimation of Arabidopsis thaliana results in incomplete recovery of photosynthetic capacity,

Posted on Authorea 21 Jul 2020 — The copyright holder is the author/funder. All rights reserved. No reuse without permission. — https://doi.org/10.22541/au.159534893.31472268 — This a preprint and has not been peer reviewed. Data may be preliminary.

associated with an increased reduction of the chloroplast stroma. *Planta, 214* (2), 295-303.

Savitch, L. V., Leonardos, E. D., Krol, M., Jansson, S., Grodzinski, B., Huner, N. P. A., & Oquist, G. (2002). Two different strategies for light utilization in photosynthesis in relation to growth and cold acclimation. *Plant Cell and Environment, 25* (6), 761-771.

Smith, A. M., & Stitt, M. (2007). Coordination of carbon supply and plant growth. *Plant Cell Environ, 30* (9), 1126-1149. doi:10.1111/j.1365-3040.2007.01708.x

Stein, O., & Granot, D. (2019). An Overview of Sucrose Synthases in Plants. *Frontiers in plant science, 10* (95). doi:10.3389/fpls.2019.00095

Stitt, M., & Hurry, V. (2002). A plant for all seasons: alterations in photosynthetic carbon metabolism during cold acclimation in Arabidopsis.*Current Opinion in Plant Biology, 5* (3), 199-206. doi:10.1016/s1369-5266(02)00258-3

Strand, A., Foyer, C. H., Gustafsson, P., Gardestrom, P., & Hurry, V. (2003). Altering flux through the sucrose biosynthesis pathway in transgenic Arabidopsis thaliana modifies photosynthetic acclimation at low temperatures and the development of freezing tolerance. *Plant Cell and Environment, 26* (4), 523-535. doi:10.1046/j.1365-3040.2003.00983.x

Strand, A., Hurry, V., Gustafsson, P., & Gardestrom, P. (1997). Development of Arabidopsis thaliana leaves at low temperatures releases the suppression of photosynthesis and photosynthetic gene expression despite the accumulation of soluble carbohydrates. *Plant Journal, 12* (3), 605-614.

Strand, A., Hurry, V., Henkes, S., Huner, N., Gustafsson, P., Gardestrom, P., & Stitt, M. (1999). Acclimation of Arabidopsis leaves developing at low temperatures. Increasing cytoplasmic volume accompanies increased activities of enzymes in the Calvin cycle and in the sucrose-biosynthesis pathway. *Plant Physiology, 119* (4), 1387-1397. doi:10.1104/pp.119.4.1387

Talts, P., Parnik, T., Gardestrom, P. e. r., & Keerberg, O. (2004). Respiratory acclimation in Arabidopsis thaliana leaves at low temperature. *Journal of Plant Physiology, 161* (5), 573-579. doi:https://doi.org/10.1078/0176-1617-01054

Walters, R. G. (2005). Towards an understanding of photosynthetic acclimation. *Journal of Experimental Botany, 56* (411), 435-447.

Walters, R. G., & Horton, P. (1994). Acclimation of *Arabidopsis thaliana* to the light environment - changes in the compostition of the photosynthetic apparatus. *Planta, 195* (2), 248-256.

Wedding, R. T., Black, M. K., & Meyer, C. R. (1990). Inhibition of phosphoenolpyruvate carboxylase by malate. *Plant Physiology, 92* (2), 456-461. doi:10.1104/pp.92.2.456

Weise, S. E., Liu, T., Childs, K. L., Preiser, A. L., Katulski, H. M., Perrin-Porzondek, C., & Sharkey, T. D. (2019). Transcriptional Regulation of the Glucose-6-Phosphate/Phosphate Translocator 2 Is Related to Carbon Exchange Across the Chloroplast Envelope.*Frontiers in plant science, 10* (827). doi:10.3389/fpls.2019.00827

Zell, M. B., Fahnenstich, H., Maier, A., Saigo, M., Voznesenskaya, E. V., Edwards, G. E., . . . Maurino, V. G. (2010). Analysis of Arabidopsis with Highly Reduced Levels of Malate and Fumarate Sheds Light on the Role of These Organic Acids as Storage Carbon Molecules. *Plant Physiology, 152* (3), 1251-1262. doi:10.1104/pp.109.151795

Figure legends

Figure 1: Maximum capacity of photosynthesis (a), measured at 20degC under CO_2- and light-saturating conditions at the end of each day of the acclimation period, for the wild-type Col-0 (circles) and the *fum2.2* mutant (triangles). Rates of net photosynthesis (b) and respiration (c) measured as CO_2exchange in growth conditions on Col-0 and *fum2.2* plants at 20degC (white) and at 4degC after the first day of transfer (dashed)

Posted on Authorea 21 Jul 2020 — The copyright holder is the author/funder. All rights reserved. No reuse without permission. — https://doi.org/10.22541/au.159534893.31472268 — This a preprint and has not been peer reviewed. Data may be preliminary.

and after seven days of transfer (grey). Error bars show standard mean error (n=3-5). Different labels on columns in (b) and (c) indicate significantly different values (ANOVA, $P<0.05$)

Figure 2: Concentrations of starch (a), fumarate (b) and malate (c) in leaves measured at the beginning (open symbols) and end (closed symbols) of the photoperiod in Col-0 (circles) and *fum2.2*(triangles) plants. Error bars show standard mean error (n=5-7).

Figure 3: Distribution of diurnally fixed carbon, calculated from Figures 1-3 and data in Dyson et al. (2016) for Col-0 (a,c) and*fum2.2* (b,f) plants in control conditions, on the first day of cold treatment (D0) and after one week of cold treatment (D7). Beginning-of-day concentrations were subtracted from end-of-day concentrations to estimate total diurnal fluxes to different sinks. Measured carbon sinks are fumarate (orange), malate (green), diurnal respiration (blue) and starch (purple). Export (and other) values (c,d) were calculated by subtracting all other values from the total diurnal carbon capture via photosynthesis. Data for "sugar", which include sucrose and glucose retained in the leaf, are included in the analysis but are not visible on the scale of this figure.

Figure 4: Total protein concentrations (a) as calculated from Bradford assays. Different labels on columns indicate significantly different values (ANOVA, $P<0.05$). Principal component analysis (b) of the log2 scaled protein intensities in leaves of Col-0 (circles) and *fum2.2* (triangles) plants measured .in control conditions (open symbols) and after one week of cold treatment (closed symbols). Hierarchical clustering and heat-map (c) of the log2 scaled protein values. Fold changes for Cluster 1 (d), 2 (e), 3 (f) and 4 (g), relative to Col-0 controls, are shown for the two genotypes and conditions. Full proteomic dataset is available in Table S1.

Figure 5: Summary of the relative abundance of proteins for the Benson-Calvin cycle enzymes of Col-0 (white bars) and *fum2.2*(grey bars) plants in control conditions (solid colours) and on Day 7 of 4degC treatment (hatched bars), as shown in the legend on the bottom left. RuBP (ribulose bisphosphate), 3PG (3-phosphoglycerate), 1,3-BPG (1,3-bisphosphoglycerate), GA3P (glyceraldehyde 3-phosphate), DHAP (dihydroxy-acetone-phosphate), SDP (sedoheptulose-1,7-bisphosphate), FBP (fructose-1,6-bisphosphate), F6P (fructose-6-phosphate), SDP (sedoheptulose-1,7-bisphosphate), S7P (sedoheptulose-1-phosphate), Ru5P (ribulose-5-phopshate), X5P (xylulose-5-phosphate). Data represent the total summed signal for all unique detected peptides in each case. Error bars represent the standard mean error, with different letters indicating significantly different values

Figure 6: The two shortest feasible pathways for producing fumarate in the cytosol, identified using a network analysis and flux sampling (see Materials and Methods for more details). The two pathways differ in the form of carbon exported from the chloroplast to the cytosol compartments. RuBP (ribulose bisphosphate), PGA (3-phosphoglyceric acid), DPGA (2,3-diphosphoglyverate), TP (triose phosphate), 2PGA (2-phosphoglycerate), PEP (phosphoenolpyruvate carboxylase), Pyr (Pyruvate), OAA (Oxaloacetate), Mal (Malate), Fum (Fumarate).

Figure 7: Flux sampling results obtained from the Col-0 (black) and *fum2.2* (red) models for the export of PGA (3-phosphoglyceric acid ; a-d) and the export of TP (triose phosphate; e-h) from the chloroplast. Models were constrained according to cold conditions (a,e), to control conditions but with the rate of photosynthesis on the first day of 4degC treatment (b,f) , to cold conditions on Day 7 of 4degC treatment (c,g) and to control conditions with the production of NADPH set to lowest feasible value (d,h). Each panel shows a frequency diagram, representing the frequency with which each solution value was achieved over repeated iterations of the modelling.

Figure 8: Seed yield in plants of wild type Col-0 and*fum2.2* grown for 8 weeks at 20°C and then either maintained at 20°C for a further 7 days (white bars), or transferred to 4°C for the same time (grey bars), before being transferred to a 16h day, to induce flowering. For each plant, the number of seeds per silique was counted for 10 siliques per plant (a) and the number of siliques counted on 6 plants (b). Total seed yield per plant was estimated as the product of these numbers (c). Error bars shown represent the standard error of the mean. Different letters on the bars indicate significantly different values (ANOVA, $P<0.05$).

Posted on Authorea 21 Jul 2020 — The copyright holder is the author/funder. All rights reserved. No reuse without permission. — https://doi.org/10.22541/au.159534893.31472268 — This a preprint and has not been peer reviewed. Data may be preliminary.

Supporting Information

Table S1: List of quantified proteins. Gene code and protein name are shown in the columns "Accession" and "Description", respectively. The number of identified peptides, which may be shared with other proteins, is shown in the column "Peptide count". Proteins were quantified only when 3 or more non-redundant constituent peptides were quantified, the number of which is shown in the column "peptides used for quantitation". After normalisation, the average relative abundance of each protein is shown. Individual comparisons between each condition are also shown, with P being less tan 0.05. Raw data available at https://github.com/HAHerrmann/FluxSampling Col0Fum2/blob/master/ExperimentalData/ProteinConc.xlsx and stored under the Zenodo DOI: 10.5281/zenodo.3366934

Figure S1: Concentrations of sucrose (a) and glucose (b) in leaves, measured at the beginning (open symbols) and end (closed symbols) of the photoperiod in Col-0 (circles) and *fum2.2*(triangles) plants. Error bars show standard mean error.

Figure S2: Summary of the enzyme concentrations of the sucrose synthesis pathway of Col-0 (white bars) and fum2.2 (grey bars) plants in control conditions (solid colours) and on Day 7 of 4degC treatment (hatched bars), as shown in the legend on the bottom left. TP (triose phosphate), FBP (fructose-1,6-bisphosphate), F6P (fructose-6-phosphate), G6P (glucose-6-phosphate), Tre6P (trehaolse-6-phosphate), G1P (glucose-1-phosphate), UDPG (uridine diphosphate glucose), S6P (sucrose-6-phosphate). Error bars represent the standard mean error, with different letters indicating significantly different values

Figure S3: Flux sampling results obtained from the wild type Col-0 (black) and *fum2* (red) models for the production of malate (a,f), fumarate (b,g), starch (c,h), export (d,i) and respiration (e,j) as predicted under control condition constraints (a-e) and seven days of 4degC conditions (f-j).

Figure 1

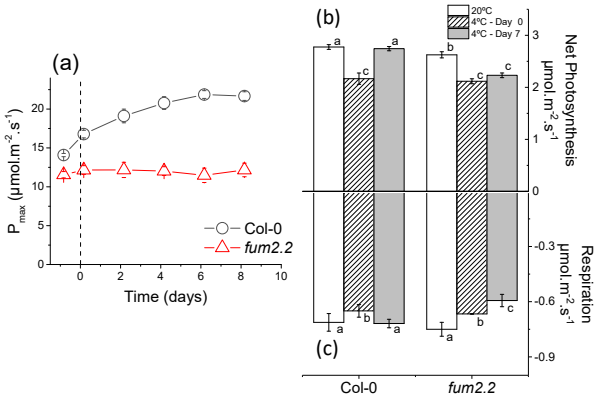

Posted on Authorea 21 Jul 2020 — The copyright holder is the author/funder. All rights reserved. No reuse without permission. — https://doi.org/10.22541/au.159534893.31472268 — This a preprint and has not been peer reviewed. Data may be preliminary.

Figure 2

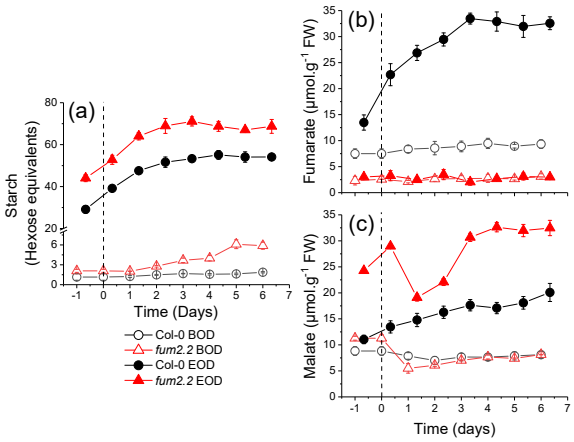

Figure 3

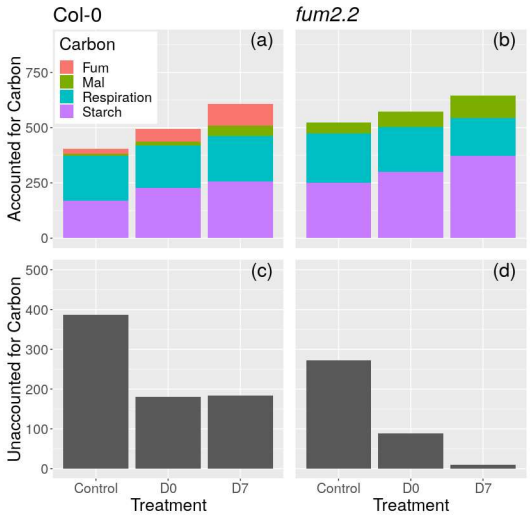

Posted on Authorea 21 Jul 2020 — The copyright holder is the author/funder. All rights reserved. No reuse without permission. — https://doi.org/10.22541/au.159534893.31472268 — This a preprint and has not been peer reviewed. Data may be preliminary.

Figure 4

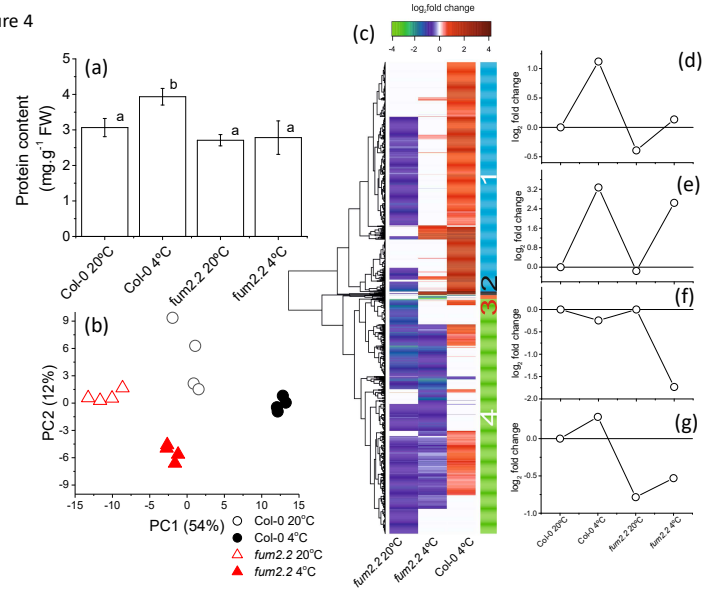

Figure 5

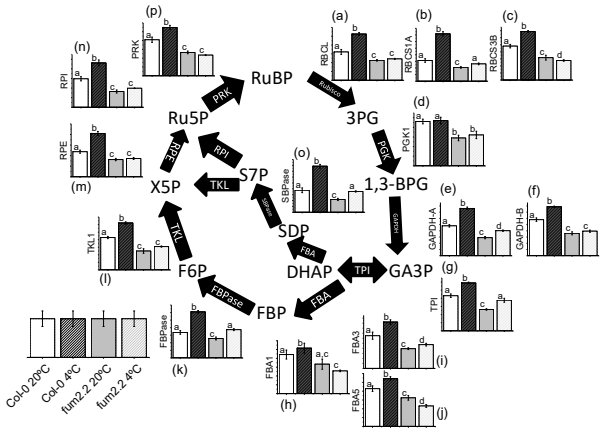

Posted on Authorea 21 Jul 2020 — The copyright holder is the author/funder. All rights reserved. No reuse without permission. — https://doi.org/10.22541/au.159534893.31472268 — This a preprint and has not been peer reviewed. Data may be preliminary.

Figure 6

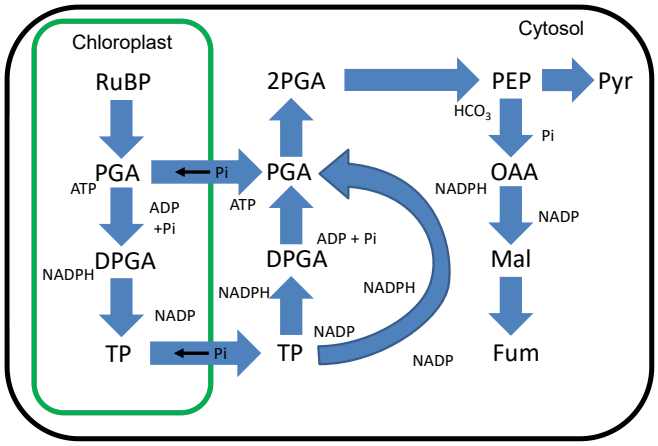

Figure 7

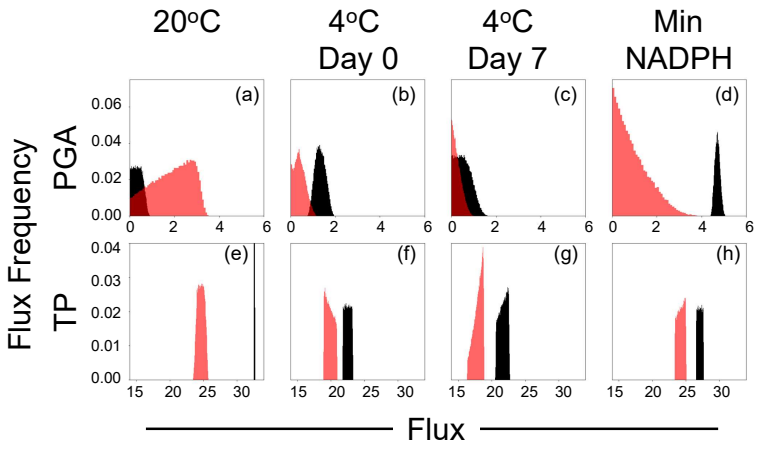

Posted on Authorea 21 Jul 2020 — The copyright holder is the author/funder. All rights reserved. No reuse without permission. — https://doi.org/10.22541/au.159534893.31472268 — This a preprint and has not been peer reviewed. Data may be preliminary.
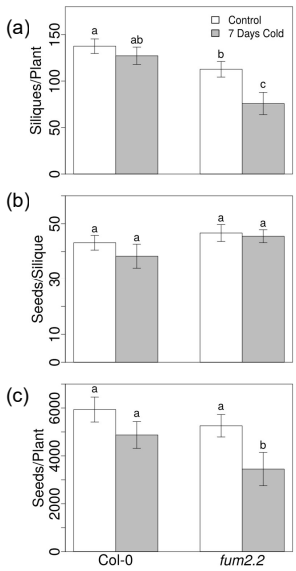
Figure 8